OPA1, encoding a dynamin-related GTPase, is mutated in autosomal dominant optic atrophy linked to chromosome 3q28

Christiane Alexander[1,2], Marcela Votruba[1,3], Ulrike E.A. Pesch[2], Dawn L. Thiselton[1], Simone Mayer[2], Anthony Moore[3,4], Miguel Rodriguez[5], Ulrich Kellner[6], Beate Leo-Kottler[7], Georg Auburger[8], Shomi S. Bhattacharya[1] & Bernd Wissinger[2]

Autosomal dominant optic atrophy (ADOA) is the most prevalent hereditary optic neuropathy resulting in progressive loss of visual acuity, centrocoecal scotoma and bilateral temporal atrophy of the optic nerve with an onset within the first two decades of life[1,2]. The predominant locus for this disorder (*OPA1*; MIM 165500) has been mapped to a 1.4-cM interval on chromosome 3q28–q29 flanked by markers *D3S3669* and *D3S3562* (ref. 3). We established a PAC contig covering the entire *OPA1* candidate region of approximately 1 Mb and a sequence skimming approach allowed us to identify a gene encoding a polypeptide of 960 amino acids with homology to dynamin-related GTPases. The gene comprises 28 coding exons and spans more than 40 kb of genomic sequence. Upon sequence analysis, we identified mutations in seven independent families with ADOA. The mutations include missense and nonsense alterations, deletions and insertions, which all segregate with the disease in these families. Because most mutations probably represent null alleles, dominant inheritance of the disease may result from haploinsufficiency of *OPA1*. *OPA1* is widely expressed and is most abundant in the retina. The presence of consensus signal peptide sequences suggests that the product of the gene *OPA1* is targeted to mitochondria and may exert its function in mitochondrial biogenesis and stabilization of mitochondrial membrane integrity.

ADOA occurs with an estimated disease prevalence of between 1:12,000 (refs 4,5) and 1:50,000 (ref. 6). The disease is highly variable in expression and shows incomplete penetrance in some families[1,2,7]. Histopathological post-mortem examination of donor eyes suggests that the fundamental pathology of ADOA is a primary degeneration of retinal ganglion cells followed by ascending atrophy of the optic nerve[8,9]. The predominant locus for ADOA was mapped to chromosome 3q28–qter (*OPA1*; refs 3,10,11), whereas linkage in a single family defined a second locus on 18q12.2–q12.3 (*OPA4*; ref. 12).

We embarked on a positional cloning approach and constructed a high-density PAC contig covering the entire *OPA1* candidate region. For the identification of candidate genes, we performed a large-scale sequence sampling on selected PACs representing the minimal tiling path for the *OPA1* interval. We localized the EST SHGC37414 to PAC H20545 (Fig. 1) and found it to be part of the Unigene cluster Hs. 147946 and the THC clusters 342414, 331187 and 379833. The corresponding full-length cDNA, KIAA0567, representing a gene of

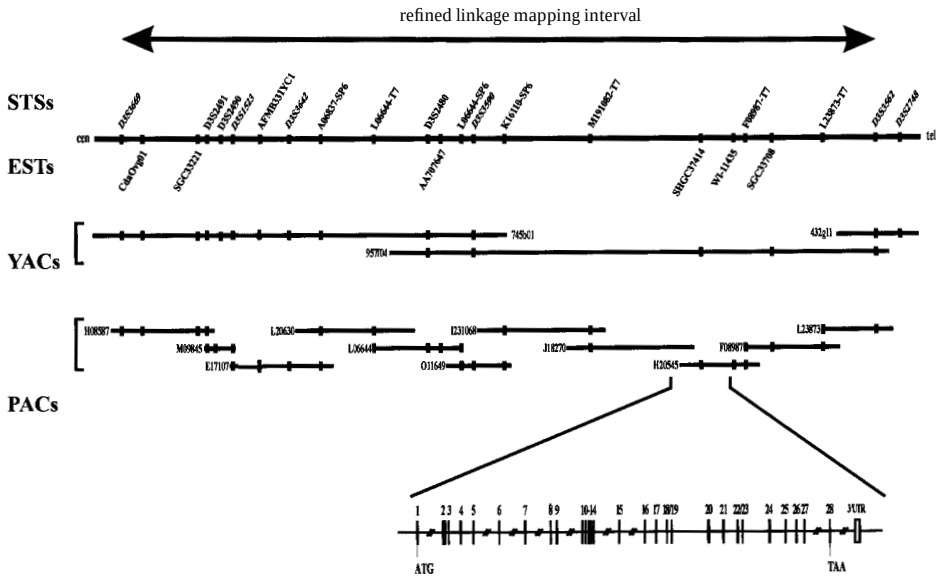

Fig. 1 Physical map of the *OPA1* interval and the genomic structure of *OPA1*. STS and EST mapping within the refined linkage mapping interval between markers *D3S3669* and *D3S3562* used to construct the physical map based on YAC and PAC clones. Vertical bars indicate the presence of STS and EST markers on the YAC and PAC clones. Only those PAC clones constituting the minimal tiling path and selected for sequence skimming are presented. Bottom, an enlarged view of the genomic structure of *OPA1* covered by PAC clones J18270 and H20545. It consists of 28 coding exons between 54 and 319 bp in length, with the initiation and stop codon (ATG, TAA) present in exon 1 and exon 28, respectively. All exon/intron boundaries follow the GT/AG rule for consensus splice-site sequences[28]. Sizes of exons and introns are drawn to scale except for introns of unknown size, indicated by double slashes on the bar. The first in-frame ATG codon is located in exon 1, leaving 56 bp of 5′ UTR sequence. The 3′ UTR is interrupted by at least one additional intron.

[1]*Department of Molecular Genetics, Insititute of Ophthalmology, University College London, London, UK.* [2]*Molecular Genetics Laboratory, University Eye Hospital, Tuebingen, Germany.* [3]*Moorfields Eye Hospital, London, UK.* [4]*Department of Ophthalmology, Addenbrookes Hospital, Cambridge, UK.* [5]*Center of Medical Genetics, Sancti-Spiritus, Cuba.* [6]*Eye Department, University Clinics Benjamin Franklin, Berlin, Germany.* [7]*Department of Pathophysiology of Vision and Neuroophthalmology, University Eye Hospital, Tuebingen, Germany.* [8]*Department of Neurology, University Hospital Duesseldorf, Germany. Correspondence should be addressed to S.S.B. (e-mail: smbcssb@ucl.ac.uk) or B.W. (e-mail: bernd.wissinger@uni-tuebingen.de).*

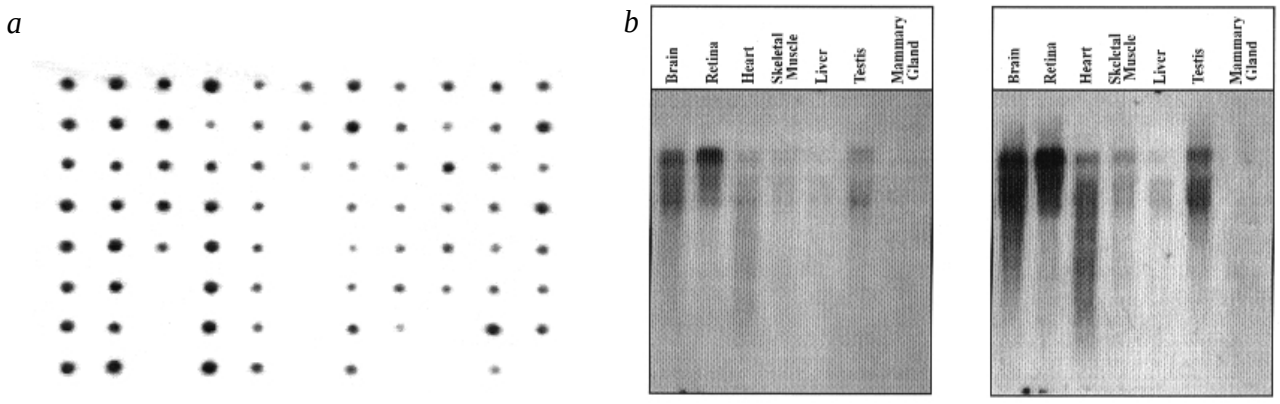

whole brain	cerebellum left	substantia nigra	heart	esophagus	colon transverse	kidney	lung	liver	leukemia HL-60	fetal brain	yeast total RNA
cerebral cortex	cerebellum right	accumbens nucleus	aorta	stomach	colon descending	skeletal muscle	placenta	pancreas	LeLa S3	fetal heart	yeast tRNA
frontal lobe	corpus callosum	thalamus	atrium left	duodenum	rectum	spleen	bladder	adrenal gland	leukemia K-562	fetal kidney	E.coli rRNA
parietal lobe	amygdala	pituitary gland	atrium right	jejunum		thymus	uterus	thyroid gland	leukemia MOLT-4	fetal liver	E.coli DNA
occipital lobe	caudate nucleus	spinal cord	ventricle left	ileum		peripheral blood leukocyte	prostate	salivary gland	Burkitt's lymphoma Raji	fetal spleen	Poly r(A)
temporal lobe	hippo-campus		ventricle right	ilocecum		lymph node	testis	mammary gland	Burkitt's lymphoma Daudi	fetal thymus	human Cot1-DNA
paracentral gyrus	medulla oblongata		inter-ventricular septum	appendix		bone marrow	ovary		adeno-carcinoma	fetal lung	human DNA 100 ng
pons	putamen		apex of the heart	colon ascending		trachea			lung carcinoma A549		human DNA 500 ng

Fig. 2 Expression pattern of *OPA1*. ***a***, Autoradiograph showing hybridization with the complete KIAA0567 cDNA against a commercial multiple tissue mRNA dot blot indicating ubiquitous expression. Order and arrangement of applied samples (ranging from 110 to 750 ng mRNA per dot) is given below. Note the absence of signals from the control samples on the right column. ***b***, Autoradiographs of 2.5 h (left) and 6 h (right) exposures of a northern blot hybridized with the complete KIAA0567 cDNA. Care was taken to apply the same amount of total RNA (6 μg each) in each lane and the tissue of origin is marked above. Transcripts of ~5.5 kb, ~4.5 kb and ~4 kb are visible. Strongest signals were present in the retina, followed by brain, heart, testis and skeletal muscle. RT–PCR experiments on liver and kidney RNA using overlapping sets of primers covering the ORF ruled out the presence of alternatively spliced transcripts (data not shown). Therefore, the shorter transcripts observed in the northern blot may result from alternative polyadenylation sites.

unknown function, had been isolated from a brain cDNA library[13]. We determined the genomic structure of this corresponding gene on the basis of comparisons of the cDNA with the genomic sequences obtained from the PAC sequencing, inter-exon PCRs and vectorette-PCR using PAC DNA as template. The coding sequence is split into 28 exons covering at least 40 kb of genomic sequence and arranged in centromere-to-telomere orientation (Fig. 1).

Northern-dot-blot hybridizations showed that KIAA0567 is ubiquitously expressed with varying abundances (Fig. 2*a*). We detected a major transcript of approximately 5.5 kb, corresponding roughly in size with the full-length cDNA, and minor species of

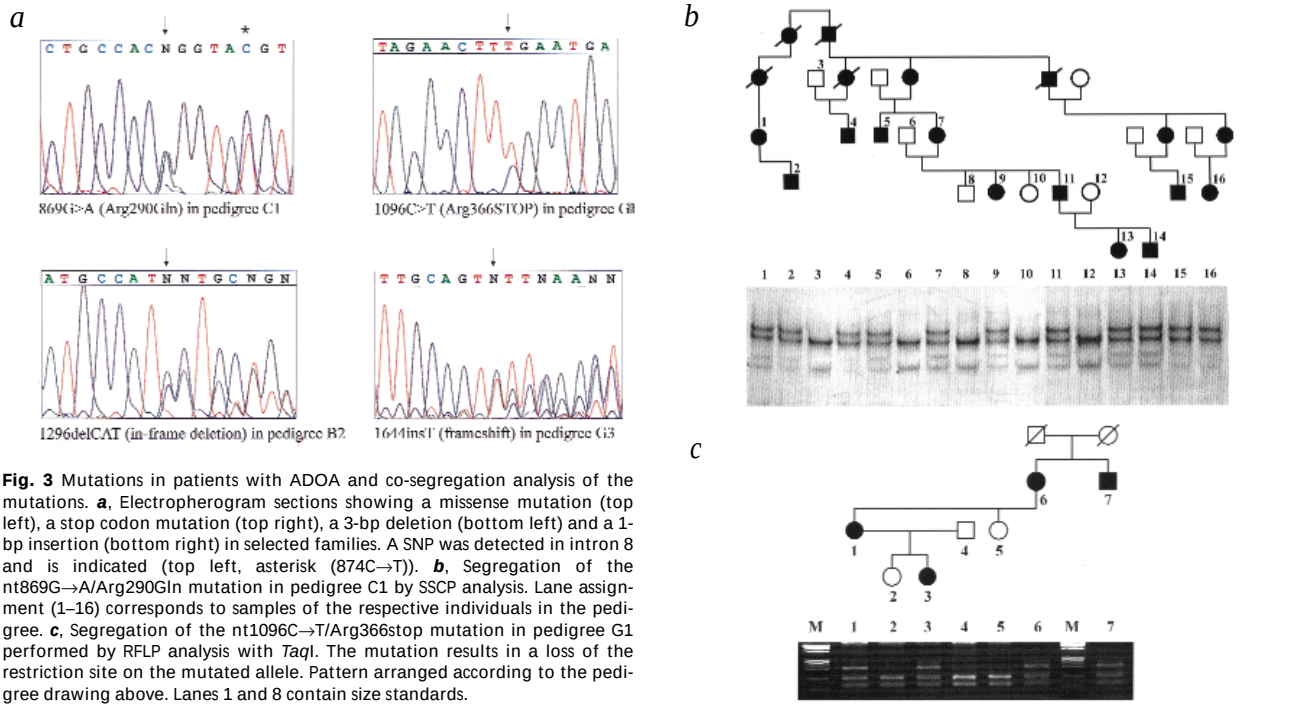

Fig. 3 Mutations in patients with ADOA and co-segregation analysis of the mutations. ***a***, Electropherogram sections showing a missense mutation (top left), a stop codon mutation (top right), a 3-bp deletion (bottom left) and a 1-bp insertion (bottom right) in selected families. A SNP was detected in intron 8 and is indicated (top left, asterisk (874C→T)). ***b***, Segregation of the nt869G→A/Arg290Gln mutation in pedigree C1 by SSCP analysis. Lane assignment (1–16) corresponds to samples of the respective individuals in the pedigree. ***c***, Segregation of the nt1096C→T/Arg366stop mutation in pedigree G1 performed by RFLP analysis with *Taq*I. The mutation results in a loss of the restriction site on the mutated allele. Pattern arranged according to the pedigree drawing above. Lanes 1 and 8 contain size standards.

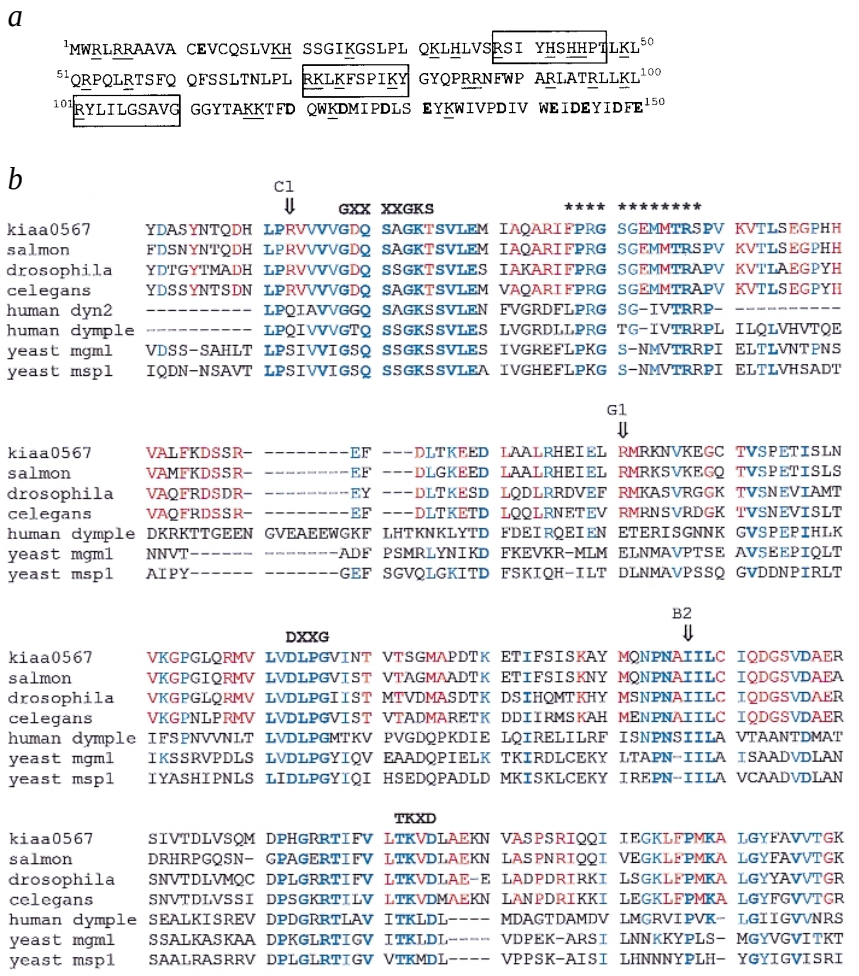

Fig. 4 Key functional features of OPA1 primary structure. ***a***, Predicted mitochondrial import signal sequence of OPA1. The first 150 amino acids of the protein sequence are shown. Basic residues (R, K, H) are underlined. Acidic residues (D, E) are printed in bold. Three putative cleavage sites (residues 38–47, 80–89, 100–109) matching the MPP/MIP consensus sequence are boxed. ***b***, Protein alignment depicting the similarity of human OPA1 with dynamin-like proteins from other species and DYN2. OPA1 shows highest homologies over its full length to salmon GTP-binding protein Mg120 expressed in motor neurons of brain[16] (75% over the entire protein), rat Rn protein (97% from residues 662 to 978), a *C. elegans* dynamin-like GTP-binding protein (48% from residues 108 to 957) and *Drosophila* CG8479 gene product (48% from residues 82 to 977). The dynamin-homologous region of OPA1 and its related proteins are shown, which consists of aa 280–520 of OPA1 (exons 7–15). The three consensus GTP-binding motifs are indicated above the alignment in bold and the dynamin signature is overscored by asterisks. Amino acid residues conserved only in putative orthologues of KIAA0567 are highlighted in red, whereas those conserved also in characterized dynamin-like proteins are depicted in blue, with those conserved across all members of the alignment in bold. Mutations altering one KIAA0567 amino acid residue found to segregate in ADOA pedigrees C1, G1 and B3 are indicated by an arrow.

approximately 4.5 and approximately 4.0 kb on northern blots (Fig. 2*b*). The highest transcript level was observed in retina, followed by brain, testis, heart and skeletal muscle. The high level of the transcript in the retina results from an increased abundance of the 5.5-kb transcript.

We screened patients from *OPA1*-linked families originating from Germany, the United Kingdom[2] and Cuba[14] by direct sequencing of coding exons. We identified 7 putative pathogenic mutations in index patients, including a non-conservative missense mutation (R290Q), a stop codon mutation (R366X), a 3-bp in-frame deletion (I432del), two 1-bp deletions (1016delC; 1354delG), a deletion resulting in the complete loss of exon 20 and a 1-bp insertion (1644insT; Fig. 3*a* and Table 1). Analysis within the individual families revealed segregation of the mutations with the disease haplotype (Fig. 3*b*). One individual with the disease mutation from each of families B3 and G2 has normal visual acuity and normal optic disc appearance, but declined detailed psychophysical and electrophysiological testing. These sequence alterations were not present in at least 50 healthy control subjects.

Examination of the amino-terminal leader sequence of the deduced protein revealed the features typical of a protein imported into the matrix space of mitochondria: an enrichment of basically charged amino acids and the presence of the MPP/MIP cleavage consensus sequence RX↓(F/L/I)XX(G/S/T)XXXX↓ (Fig. 4*a*; ref. 15). OPA1 shows highest identity scores over the whole length to dynamin-related large GTPases from salmon[16], *Caenorhabditis elegans* and *Drosophila melanogaster*, and the RN protein (Fig. 4*b*). The carboxy terminus of OPA1 differs from that of other dynamin family members in lacking a proline-rich region, a GED domain and a pleckstrin homology domain, which may determine the specific functions of the protein[17,18]. The GTPase domain, encompassing the core central region between amino acid residues 280 and 520, harbours the consensus tripartite GTP-binding motif needed for phosphate binding (GXXXXGKS/T), coordination of Mg^{2+} (DXXG), nucleotide binding (T/NKXD) and the dynamin sequence signature, which are characteristically conserved in dynamin-related GTPases[19]. Apart from DynI, DynII and DynIII, only one dynamin-related large GTPase, Drp1, has been identified in mammalian cells. This protein is located within the cytoplasm and controls mitochondrial distribution and vesicular transport[20,21]. Studies in yeast have demonstrated that the dynamin-related large GTPases Dnm1, Mgm1 and Msp1 (refs 22–24) have an important role in the maintenance and inheritance of mitochondria. OPA1 shows greatest similarity at the primary level to Mgm1 (Fig. 4*b*).

The preponderance of protein-truncation mutations in *OPA1* suggests that the pathophysiological basis of ADOA may rely on the

Table 1 • Mutations detected in *OPA1*

Family	Origin	exon/intron	Nucleotide alteration*	Predicted change
C1	Cuba	exon 8	869G>A	Arg290Gln
B1	UK	exon 10	1016delC	frameshift, 19 novel aa then STOP
G1	Germany	exon 11	1096C>T	Arg366STOP
B2	UK	exon 13	Del1296CAT	Del432Ile
G2	Germany	exon 14	1354delG	frameshift, 14 novel aa then STOP
G3	Germany	exon 17	1644insT	frameshift, 12 novel aa then STOP
B3	UK	exon 20	deletion of entire exon	frameshift, 13 novel aa then STOP

*Nucleotide designation commencing 1 at position 56 (translation start) of GenBank entry AB011139.

functional loss of one allele and may thus result from haploinsufficiency. Taking into account the high level of expression of *OPA1* in the retina, loss of one allele may decrease transcript level to a critical threshold in this tissue, which may explain the restricted ocular phenotype. We did not notice substantial phenotypical differences between families with protein truncating mutations and those with missense mutations, but the small number of families studied precludes meaningful conclusions. Incomplete penetrance may occur in some families with ADOA and complicate genetic counselling[1,2,7]. The cloning of *OPA1* now allows molecular genetic diagnosis and identification of asymptomatic 'at-risk' family members. Moreover, detailed psychophysical and electrophysiological investigation of those gene carriers will determine whether true incomplete penetrance or subtle ganglion cell dysfunction, indicating mild expression of the disease, applies.

The pathophysiology and clinical symptoms observed in ADOA show overlap with those occurring in Leber's hereditary optic neuropathy[25]. This disease is caused by mutations in mtDNA-encoded genes for subunits of complex I of the respiratory chain[26]. These mutations are believed to lead to insufficient energy supply in the highly energy-demanding neurons of the optic nerve (notably the papillomacular bundle) and to cause blindness by a compromise of axonal transport in retinal ganglion cells. Moreover, experimental work done in yeast indicates that impaired regulation of mitochondrial integrity can lead to loss of mitochondrial DNA and compromise respiratory competence[22]. We thus hypothesize that mutations in *OPA1* affect mitochondrial integrity resulting in an impairment of energy supply. In the long term, this may affect normal metabolic processes in retinal ganglion cells and consequently their survival. Future biochemical and sub-cellular localization studies will be essential to understanding the function of OPA1 and the pathological mechanisms leading to ADOA.

Methods

Patients, families and samples. Patients and families were recruited in different clinical centres (Ethical Committee Approval 0181 at Moorfields Eye Hospital, UK and Approval 159/98 of the Ethik-Kommission of the Medical Faculty Tuebingen, Germany). The diagnosis of ADOA was based on ophthalmological examination including visual acuity, visual field and colour testing, fundoscopy, electrophysiology and family history[2]. We took venous blood samples after informed consent and extracted DNA according to standard procedures.

PAC analysis and sequence sampling. We isolated PAC DNA using the alkaline lysis method and determined the insert sizes by pulsed-field gel electrophoretic separation of *Not*I-digested PAC DNA on a CHEF-DRIII system (Biorad). For random subcloning, we sonicated PAC DNA (10 µg) for 3×20 s with a Bandelin HD-70 sonicator, repaired the ends by treatment with T4 DNA polymerase and Klenow fragment in the presence of dNTPs (200 µM), and size-selected fragments on agarose gels before ligation with *Sma*I linearized, dephosphorylated pUC19. We used the ligations for electro-transformation of *Escherichia coli* DH10B and selected clones on IPTG/X-Gal/ampicillin plates. We prepared subclone DNA from 1-ml cultures on a BioRobot 9600 (Qiagen) and sequenced with standard M13 forward/reverse primers using Big Dye Terminator chemistry (PE Biosystems). Sequences were on an ABI377 DNA sequencer and we used the Staden Software Package[27] for editing and assembling the raw data into sequence contigs. For database searches we used BLAST at NCBI and the NIX application at the UK-HGMP.

Genomic structure of *OPA1*. We identified exons and exon/intron boundaries by analysis of sequences obtained from the original PAC sequence sampling with the KIAA0567 cDNA as query. For exon sequences not covered by the sequence sampling approach, we performed inter-exon PCR with primers designed from the cDNA sequence applying the Expand Long Template PCR System (Boehringer). Amplification was performed with DNA of the PAC clones H20545 and J18270 as templates and products directly sequenced using the PCR primers. For the remaining exons, we established vectorette libraries from PAC DNA digested with several blunt-end and 5´ overhang generating restriction endonucleases. We performed nested PCR applying primers designed from the cDNA sequence and vectorette primers and sequenced the gel-purified PCR products.

Mutation screening and co-segregation analysis. We amplified coding exons from patient genomic DNA with primers located in flanking intron and UTR sequences performing standard 50-µl PCR (in 10 mM Tris, pH 8.9, 50 mM KCl, 1.5–3 mM $MgCl_2$, 10 pmol of each primer and 200 µM each dNTP including 50–100 ng DNA and 1 U AmpliTaq polymerase). Cycling parameters were 4 min at 94 °C, 35 cycles of 30 s at 94 °C, 30 s at 53 °C and 30 s at 72 °C and a final 7 min extension at 72 °C. We purified the PCR products either by ultrafiltration (Centricon-100 cartridges, Amicon) or Qiaquick columns (Qiagen) and sequenced the samples using Big Dye Terminator chemistry. We edited and aligned the sequences using the Lasergene Software package (DNASTAR). Co-segregation analysis and screening of controls was carried out by simple PCR amplification (deletion of exon 20 in pedigree B3), PCR/RFLP analysis (nt1096C>T/Arg366stop, loss of a *Taq*I site in pedigree G1; nt1354delG/frameshift, loss of a *Tth111*I site in pedigree G2) or PCR/SSCP analysis. For SSCP we separated samples on 10% non-denaturing polyacrylamide gels containing 10% glycerol for 20 h at 4 °C and used silver staining for visualization.

Northern-blot and RNA dot-blot hybridization. We used a Human Multiple Tissue mRNA Dot Blot (Clontech) and total RNA from human brain, heart, skeletal muscle, liver, testis and mammary gland (Clontech). In addition, we isolated total human retinal RNA from donor eyes using Trizol Reagent (Gibco). We separated total RNA (6 µg each; adjusted by photometric measurement and a control gel) on a 1% agarose 2.2 M formaldehyde/MOPS gel and blotted onto a Hybond-N nylon membrane (Amersham). We labelled the insert of the full-length KIAA0567 cDNA clone with α-^{32}P-dCTP using the NEBlot kit (New England Biolabs) and hybridized the probe in ExpHyb solution (Clontech) for 15 h at 65 °C. Post-hybridization washes were done twice in 1×SSC, 0.15% SDS at 40 °C and 0.1×SSC, 0.15% SDS at 65 °C. Finally, we exposed the blots against X-ray films for 3–24 h at –80 °C with intensifying screens.

RT–PCR. Human kidney and liver RNA (1 µg) were random primed and reverse-transcribed into single-stranded cDNA with AMV Reverse Transcriptase according to the manufacturer's recommendations (RNA PCR kit, Takara) and used for PCR amplification with overlapping primer pairs covering the complete coding sequence of *OPA1*. We analysed the PCR products on agarose gels and verified their identity by DNA sequencing.

Accession numbers. KIAA0567 mRNA, GenBank AB011139. Protein accession numbers: KIAA0567 protein, BAA25493; salmon GTP-binding protein, BAA32279; *Drosophila* CG8479 gene product, AAF58275; *C. elegans* GTP-binding protein, CAA87771; human dynamin 2, NP_004936; human dynamin-like protein Dymple isoform, AAC35283; yeast Mgm1, P32266; yeast Msp1, CAA69196.

Acknowledgements

We thank all clinicians who referred patients; the patients and their family members for participation; T. Nagase for the KIAA0567 full-length cDNA clone; B. Jurklies and H. Wilhelm for the collection of additional families; C. Willis for help with UK pedigree and sample collection; B. Baumann and S. Tippmann for technical assistance; S. Kohl for help with the SSCP analysis; and C. Pusch for various technical and computational advice. This work was supported by The Wellcome Trust, UK Project Grant 056047 (M.V., S.S.B. and A.M.), The Guide Dogs for the Blind Association, The Joint British Council/DAAD Academic Research Collaboration Programme ARC 1074 (M.V. & B.W.), and a grant from the Bundesministerium fuer Bildung und Forschung (01 KS 9602) and the Interdisziplinaeres Zentrum fuer Klinische Forschung Tuebingen (B.W.). C.A. is supported by a fellowship of the Deutsche Forschungsgemeinschaft.

Received 12 April; accepted 14 August 2000.

1. Hoyt, C.S. Autosomal dominant optic atrophy. A spectrum of disability. *Ophthalmology* **87**, 245–251 (1980).
2. Votruba, M. *et al.* Clinical features in affected individuals from 21 pedigrees with dominant optic atrophy. *Arch. Ophthalmol.* **116**, 351–358 (1998).
3. Jonasdottir, A., Eiberg, H., Kjer, B., Kjer, P. & Rosenberg, T. Refinement of the dominant optic atrophy locus (OPA1) to a 1.4-cM interval on chromosome 3q28–3q29, within a 3-Mb YAC contig. *Hum. Genet.* **99**, 115–120 (1997).
4. Kivlin, J.D., Lovrien, E.W., Bishop, D.T. & Maumenee, I.H. Linkage analysis in dominant optic atrophy. *Am. J. Hum. Genet.* **35**, 1190–1195 (1983).
5. Kjer, B., Eiberg, H., Kjer, P. & Rosenberg, T. Dominant optic atrophy mapped to chromosome 3q region. II. Clinical and epidemiological aspects. *Acta Ophthalmol. Scand.* 1996 **74**, 3–7 (1996).
6. Lyle, W.M. *Genetic Risks* (University of Waterloo Press, Waterloo, Ontario, 1990).
7. Johnston, R.L., Seller, M.J., Behnam, J.T., Burdon, M.A. & Spalton, D.J. Dominant optic atrophy. Refining the clinical diagnostic criteria in light of genetic linkage studies. *Ophthalmology* **106**, 123–128 (1999).
8. Johnston, P.B., Gaster, R.N., Smith, V.C. & Tripathi, R.C. A clinicopathologic study of autosomal dominant optic atrophy. *Am. J. Ophthalmol.* **88**, 868–875 (1979).
9. Kjer, P., Jensen, O.A. & Klinken, L. Histopathology of eye, optic nerve and brain in a case of dominant optic atrophy. *Acta Ophthalmol. (Copenh)* **61**, 300–312 (1983).
10. Eiberg, H., Kjer, B., Kjer, P. & Rosenberg, T. Dominant optic atrophy (OPA1) mapped to chromosome 3q region. I. Linkage analysis. *Hum. Mol. Genet.* **3**, 977–980 (1994).
11. Brown, J. *et al.* Clinical and genetic analysis of a family affected with dominant optic atrophy. *Arch. Ophthalmol.* **115**, 95–99 (1997).
12. Kerrison, J.B. *et al.* Genetic heterogeneity of dominant optic atrophy, Kjer type: identification of a second locus on chromosome 18q12.2–12.3. *Arch. Ophthalmol.* **117**, 805–810 (1999).
13. Nagase, T. *et al.* Prediction of the coding sequences of unidentified human genes. XII. The complete sequences of 100 new cDNA clones from brain which code for large proteins in vitro. *DNA Res.* **5**, 355–364 (1998).
14. Lunkes *et al.* Refinement of the OPA1 gene locus on chromosome 3q28–q29 to a region of 2-8 cM, in one Cuban pedigree with autosomal dominant optic atrophy Type Kjer. *Am. J. Hum. Genet.* **57**, 968–970 (1995).
15. Branda, S. *et al.* Yeast and human frataxin are processed to mature form in two sequential steps by the mitochondrial processing peptidase. *J. Biol. Chem.* **274**, 22763–22769 (1999).
16. Kubakawa, K., Miyashita, T. & Kubo, Y. Isolation of a cDNA for a novel 120-kDa GTP-binding protein expressed in motor neurons in the salmon brain. *FEBS Lett.* **431**, 231–235 (1998).
17. Muhlberg, A.B., Warnock, D.E. & Schmid, S.L. Domain structure and intramolecular regulation of dynamin GTPase. *EMBO J.* **16**, 6676–6683 (1997).
18. McNiven, M.A., Cao, H., Pitts, K.R. & Yoon, Y. The dynamin family of mechanoenzymes: pinching in new places. *Trends Biochem. Sci.* **25**, 115–120 (2000).
19. Guan, K., Farh, L., Marshall, T.K. & Deschenes, R.J. Normal mitochondrial structure and genome maintenance in yeast requires the dynamin-like product of the MGM1 gene. *Curr. Genet.* **24**, 141–148 (1993).
20. Kamimoto, T. *et al.* Dymple, a novel dynamin-like high molecular weight GTPase lacking a proline-rich carboxyl-terminal domain in mammalian cells. *J. Cell. Biol. Chem.* **273**, 1044–1051 (1998).
21. Smirnova, E., Shurland, D.L., Ryazantsev, S.N. & van der Bliek, A.M. A human dynamin-related protein controls the distribution of mitochondria. *J. Cell Biol.* **143**, 351–358 (1998).
22. Shepard, K.A. & Yaffe, M.P. The yeast dynamin-like protein, Mgm1p, functions on the mitochondrial outer membrane to mediate mitochondrial inheritance. *J. Cell Biol.* **144**, 711–720 (1999).
23. Bleazard, W. *et al.* The dynamin-related GTPase Dnm1 regulates mitochondrial fission in yeast. *Nature Cell Biol.* **1**, 298–304 (1999).
24. Pelloquin, L., Belenguer, P., Menon, Y. & Ducommun, B. Identification of a fission yeast dynamin-related protein involved in mitochondrial DNA maintenance. *Biochem. Biophys. Res. Commun.* **251**, 720–726 (1998).
25. Riordan-Eva, P. *et al.* The clinical features of Leber's hereditary optic neuropathy defined by the presence of a pathogenic mitochondrial mutation. *Brain* **118**, 319–337 (1995).
26. Wallace, D.C. *et al.* Mitochondrial DNA mutations associated with Leber's hereditary optic neuropathy. *Science* **242**, 1427–1430 (1988).
27. Staden, R., Beal, K.F. & Bonfield, J.K. The Staden package, 1998. *Methods Mol. Biol.* **132**, 115–130 (2000).
28. Breathnach, R. & Chambon, P. Organization and expression of eukaryotic split genes coding for proteins. *Annu. Rev. Biochem.* **50**, 349–383 (1981).